Segmentation of Soil µCT Images

Pore–Solid Phase Separation

Introduction to Image Processing and Analysis (71254)

Date: 01/02/2026

Authors:

Rony Schwartz and Denis Neuman

Introduction

Soil is not merely a physical substrate but a complex porous medium in which the internal pore structure governs fundamental processes such as water flow, aeration, and nutrient transport. Consequently, quantitative characterization of soil pore space is essential for advancing agricultural and environmental research.

Micro–computed tomography (µCT) is a non-destructive, high-resolution imaging technique that enables detailed visualization of the internal soil structure, including both air-filled pore space and the mineral solid phase, without disturbing the sample. This technology allows direct extraction of pore-scale structural information from three-dimensional soil images.

From binary segmentation of pore and solid phases, it is possible to derive meaningful structural metrics that are directly related to soil hydraulic behavior, such as total porosity, pore size distribution, basic pore connectivity, and surface-to-volume ratio.

Moreover, pore size distributions derived from µCT images can be used to indirectly estimate the soil water retention curve, by linking pore radii to capillary pressure through physical models. Such an approach provides a structural interpretation of soil water retention, although it relies on simplifying assumptions and does not replace direct laboratory measurements.
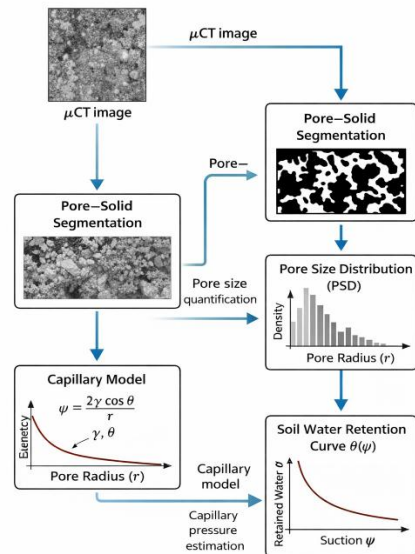

Figure 1. Workflow for estimating soil water retention behavior from µCT-derived pore structure

Recent studies have demonstrated that classical intensity-based segmentation methods often fail in complex soil µCT images due to overlapping grayscale distributions and structural heterogeneity. In contrast, deep learning approaches based on convolutional neural networks (CNNs) have shown improved performance in segmenting soil constituents in µCT data, particularly for complex and low-contrast structures.

In this work, we evaluate the performance of classical automatic segmentation using Otsu thresholding as a baseline approach for pore–solid separation in soil µCT images, and discuss its role in the context of more advanced learning-based segmentation methods.

Database

The database consists of grayscale µCT images of soil, obtained from an ongoing soil physics research project. The data represent the internal structure of soil samples, including both the mineral solid phase and the air-filled pore space.

The dataset includes approximately 8,000 two-dimensional image slices, extracted from three-dimensional µCT scans and stored in TIFF image format. The original images were acquired with a 16-bit depth, allowing a wide dynamic range of grayscale intensities.

The slices originate from different regions within the soil samples and include data from three different soil types, enabling comparative analysis across varying soil structures.

The dataset is unpublished and used exclusively for academic and educational purposes within the framework of the course.
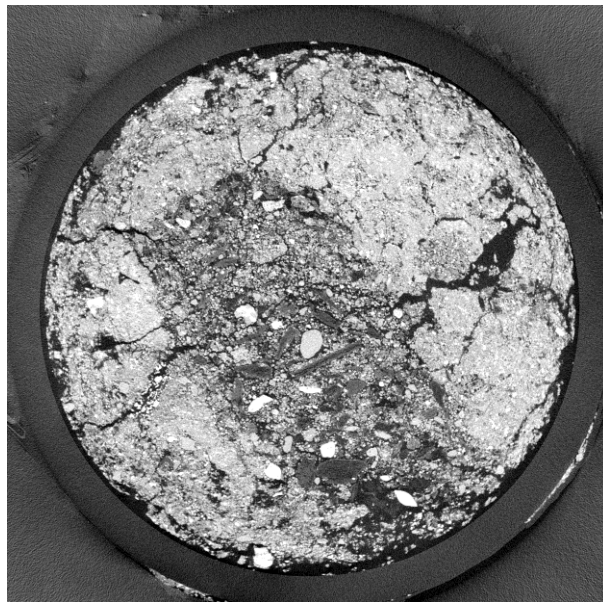

Figure 2. Example µCT image slice from the soil dataset acquired at Mishmar HaNegev (pixel size: 5.8 µm)

Methods

Image Reconstruction and Quality Control

The µCT images were obtained following standard reconstruction procedures. All reconstructed slices were visually inspected to identify potential reconstruction errors, including ring artifacts and other imaging artifacts that could affect subsequent analysis. Slices exhibiting severe artifacts were excluded from further processing.

Intensity Normalization and Bit-Depth Conversion

To ensure consistency across the dataset, intensity normalization was applied to all images. Specifically, all slices were normalized to a fixed maximum grayscale intensity value of 200. Following normalization, the images were converted from the original 16-bit representation to a consistent 8-bit format, facilitating uniform processing and compatibility with segmentation methods.

Noise Reduction

To reduce the effect of noise while preserving the main structural features of the pore–solid system, median (round kernel r=5) and CLAHE (square kernel n=61) filtering was applied to the normalized images. This step was primarily intended to suppress salt-and-pepper noise commonly observed in µCT data. The median preserves edges better than gaussian blur, and the clahe improves the contrast of a pixel with its close neighbors.

Segmentation and Ground Truth Generation

Automatic segmentation was applied to separate air-filled pore space from mineral solid material in the µCT images. Multi-Otsu thresholding was used to generate a three-class (pore–interface–solid) segmentation mask based on grayscale intensity separation.
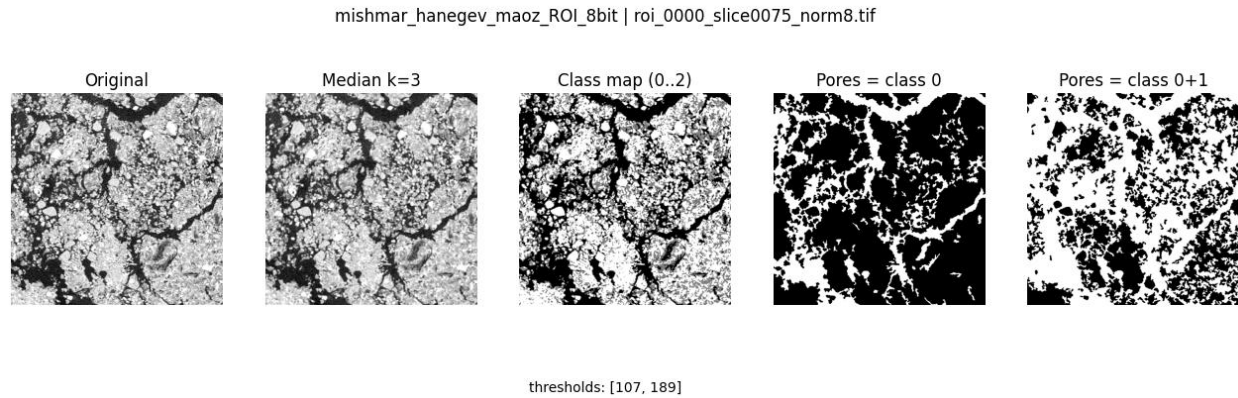
thresholds: [107, 189]

Figure 3. Example of automatic pore–solid segmentation using Otsu thresholding

Z-stability pipeline overview

The Z-stability pipeline operates on a 3D segmentation mask and evaluates segmentation consistency along the Z-axis. The volumetric mask is loaded, voxel counts per class are reported, and all subsequent analyses are performed directly on the 3D stack.

Z-local metrics computation

Z-local stability metrics are computed using both short and long sliding windows along the Z-axis. For each voxel, the pipeline measures class frequency (the fraction of voxels belonging to the target class within the window), flip rate (the number of class transitions between consecutive slices), and local pore and solid fractions, while accounting for the effective window size.

Conservative and aggressive corrections

Based on these metrics, two correction strategies are applied. In the conservative mode, a voxel is flagged as noise only if all predefined conditions are violated, including low short-range frequency, low long-range frequency, high flip rate, and small 2D component size. In

the aggressive mode, a voxel is flagged as noise if any single condition is violated. Corrected masks are saved and compared to the original segmentation.

Z-axis stability evaluation

Segmentation stability is quantified using the Dice similarity coefficient computed between adjacent slices, as well as Z-run-length stability, defined as the maximum length of consecutive voxels belonging to the target class along each vertical (Z) column. Mean and median run-length values are reported.

Pore Size Distribution (PSD) Analysis

The pore size distribution (PSD) module quantifies the distribution of pore diameters within the segmented 3D pore space. PSD is a key structural descriptor of soil, directly linked to hydraulic behavior such as water retention and flow properties. By characterizing how pore volume is distributed across different diameters, the PSD provides a structural basis for interpreting soil hydraulic functions.

PSD was computed following the morphological granulometry framework proposed by Vogel et al. An anisotropic Euclidean Distance Transform (EDT) was first applied to the binary pore volume, accounting for voxel spacing. A voxel-wise morphological opening using spherical structuring elements was then performed to determine the maximal inscribed sphere at each pore voxel. The resulting local pore diameters were aggregated into cumulative and differential PSD curves through histogram binning.

To ensure methodological consistency, the analysis followed the constraints defined by Vogel et al. : pores intersecting image borders were excluded, a reliability threshold of 5 voxels was applied to account for resolution limits. Pore size was defined as the hydraulic diameter corresponding to the largest inscribed sphere.

Results

Z-stability Analysis Summary

The Z-stability analysis of μCT scans for three soil types (Rehovot, Mishmar HaNegev, and Bnei Reem) evaluated segmentation consistency along the vertical axis using Dice coefficients and run-length metrics.
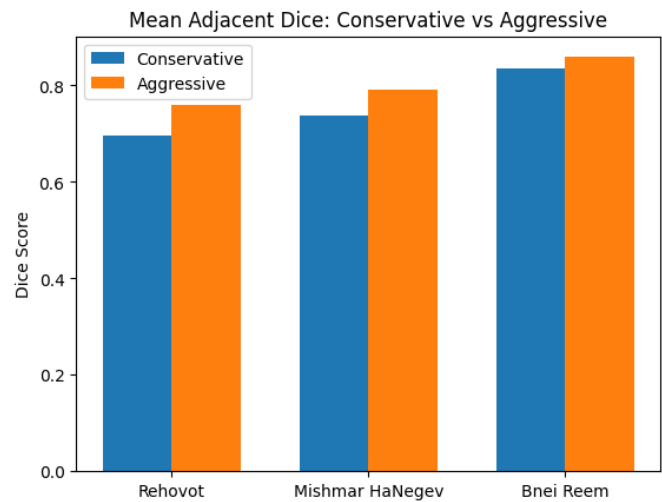

Figure 4. Mean Adjacent Dice Coefficient under Conservative and Aggressive Z-Stability Correction
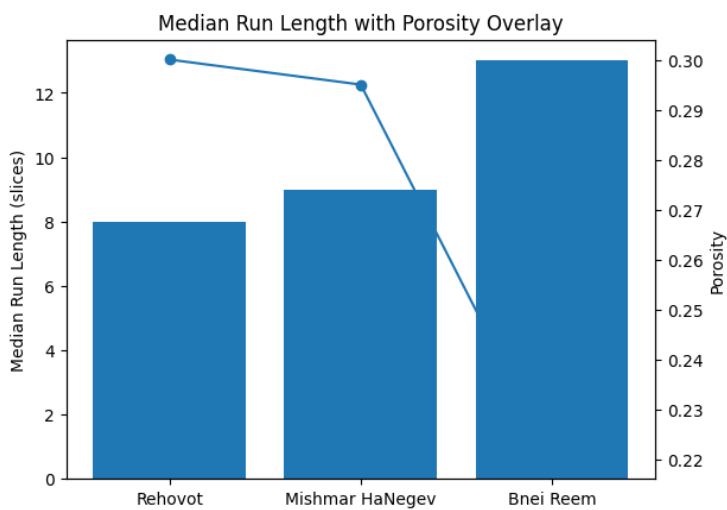

Figure 5. Median Vertical Run-Length with Porosity Overlay

Consistency: All datasets showed high inter-slice similarity. Stability was highest in Bnei Reem (vertisol) and lowest in Rehovot (sandy loam), with Mishmar HaNegev (loess) in between.

Configurations: The "aggressive" setting increased vertical coherence and Dice values by correcting more voxels, while the "conservative" setting focused on preserving the original segmentation by correcting only major inconsistencies.
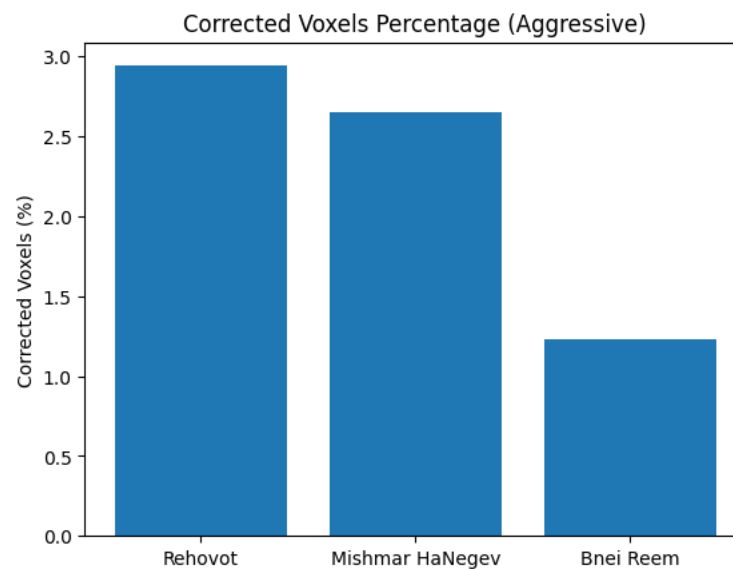

Figure 6. Percentage of Corrected Voxels under Aggressive Z-Stability Mode

Structural Continuity: High median run-lengths confirmed that segmented regions remain vertically persistent across multiple slices, particularly in the Bnei Reem sample.

Pore Size Distribution (PSD) Analysis

The PSD analysis revealed clear structural differences between the three soil samples within the reliable diameter range (≥5 voxels). Rehovot exhibited a markedly broader

distribution, extending to larger equivalent pore diameters and reaching the highest maximum diameter values among the datasets.

Mishmar HaNegev showed a pore size distribution dominated by small to intermediate pore classes, with a relatively narrower diameter range. In contrast, Bnei Reem displayed a more compact distribution, with a lower contribution of large pore classes within the reliable range. The broader range observed in Rehovot was accompanied by higher overall porosity and a stronger contribution of large pore classes, indicating a more heterogeneous pore architecture. The number of reliable bins was also highest in Rehovot, reflecting greater structural variability across scales.

Overall, the PSD results indicate distinct pore-network characteristics between the sandy loam, loess, and vertisol samples, with decreasing large-pore contribution and structural variability from Rehovot to Bnei Reem.
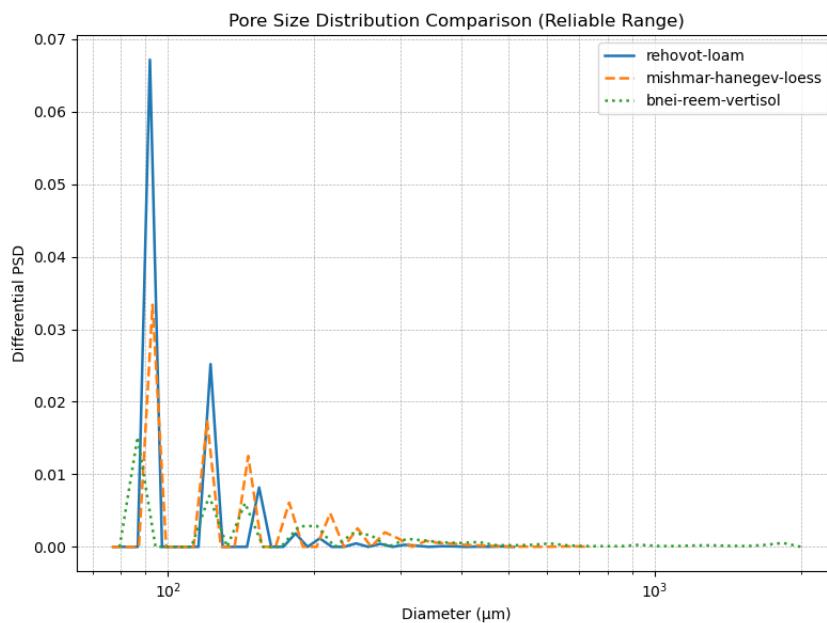

Figure 7. Differential Pore Size Distribution (PSD) in the Reliable Diameter Range (≥ 5 Voxels)

Discussion

The pore size distribution (PSD) analysis revealed clear structural differences between the three soil types. The Rehovot brown-red sandy loam exhibited the highest apparent porosity and the broadest PSD, with a dominant contribution of larger pore diameters. This behavior is consistent with the expected structure of coarse-textured soils, where larger particles create intergranular macropores. The distribution indicates a well-developed pore network spanning multiple diameter scales.

In contrast, the Mishmar HaNegev loess soil showed a narrower PSD dominated by smaller pore diameters. This trend is consistent with its finer texture and higher clay and silt fractions, which typically promote the formation of micropores rather than macropores. However, the overall segmented porosity was lower than might be expected from physical soil data, suggesting that the segmentation process may have underestimated part of the fine pore space.

The Bney Re'em alluvial soil unexpectedly exhibited the lowest apparent porosity among the three soils. From a pedological perspective, alluvial soils are not expected to have such limited pore space. Since porosity in this study is derived directly from binary segmentation, this discrepancy likely reflects segmentation limitations rather than true structural differences. Possible causes include insufficient grayscale contrast, partial volume effects at small pore scales, and scanning under relatively wet conditions, all of which can reduce pore detectability when using global Otsu thresholding. Because the PSD is fully dependent on the segmented volume, any under-segmentation directly propagates into the calculated pore size distribution.

Overall, while the relative PSD trends reflect expected textural differences between sandy and fine-textured soils, the quantitative results must be interpreted cautiously. The analysis highlights the strong dependence of structural metrics on segmentation quality

and image conditions. Future improvements in thresholding strategy or moisture control during scanning could significantly enhance the reliability of pore-scale characterization.

We attempted to rerun the full processing pipeline using a simplified two-class (pore–solid) segmentation without applying the Z-stability stage, in order to obtain a clean benchmark baseline for comparison. The intention was to evaluate the raw Multi-Otsu segmentation performance independently of any Z-axis consistency corrections and to quantify the contribution of the stability module to the final pore structure metrics. However, due to structural dependencies within the current pipeline implementation, the workflow does not execute smoothly when the Z-stability stage is bypassed. As a result, we were unable to complete this benchmark experiment within the available time frame. Although the idea was considered during the project design phase, technical constraints and time limitations prevented its full implementation.

Conclusions

- Automatic pore–solid segmentation of soil μCT images was successfully implemented using Multi-Otsu thresholding, providing a reproducible baseline for structural analysis.
- Preprocessing and post-processing steps, particularly Z-stability correction, significantly improved vertical segmentation consistency and structural coherence.

- Z-stability metrics (Dice similarity and run-length analysis) proved effective for quantitative evaluation of segmentation reliability along the vertical axis.

- PSD analysis revealed clear structural differences between sandy loam, loess, and vertisol soils, reflecting varying structural heterogeneity and variation in large-pore contribution.

- Structural and hydraulic interpretations derived from PSD are strongly dependent on segmentation quality, highlighting the importance of threshold selection and image acquisition conditions.

- Limitations related to grayscale contrast, partial volume effects, and moisture conditions may lead to underestimation of fine pore space.

- The developed pipeline provides a comprehensive framework for integrating segmentation stability assessment with pore-scale structural characterization and can serve as a foundation for future hydraulic modeling studies.

Bibliography

Phalempin, M., Krämer, L., Geers-Lucas, M., Isensee, F., & Schlüter, S. (2021).
Deep learning segmentation of soil constituents in 3D X-ray CT images.
Geoderma, 404, 115351.

Otsu, N. (1979).
A threshold selection method from gray-level histograms.
IEEE Transactions on Systems, Man, and Cybernetics, 9(1), 62–66.

van Genuchten, M. T. (1980).
A closed-form equation for predicting the hydraulic conductivity of unsaturated soils.
Soil Science Society of America Journal, 44(5), 892–898.

Vogel, H. J., Weller, U., & Schlüter, S. (2010).
Quantification of soil structure based on Minkowski functions.
Computers & Geosciences, 36(10), 1236–1245.